Materials Science & Engineering A 797 (2020) 140075

Contents lists available at ScienceDirect

Materials Science & Engineering A

journal homepage: http://www.elsevier.com/locate/msea

The effect of the initial microstructure of the X70 low-carbon microalloyed steel on the heat affected zone formation and the mechanical properties of laser welded joints

A.I. Gordienko [a,*], L.S. Derevyagina [a], A.G. Malikov [b], A.M. Orishich [b], N.S. Surikova [a], M. N. Volochaev [c,d]

[a] Institute of Strength Physics and Materials Science of Siberian Branch Russian Academy of Sciences, 2/4, Pr. Akademicheskii, Tomsk, 634055, Russia
[b] Khristianovich Institute of Theoretical and Applied Mechanics of the Siberian Branch of the Russian Academy of Sciences, 4/1, Institutskaya str., Novosibirsk, 630090, Russia
[c] Kirensky Institute of Physics of the Siberian Branch of the Russian Academy of Sciences (SB RAS), Akademgorodok 50, bld. 38, Krasnoyarsk, 660036, Russia
[d] Reshetnev Siberian State University of Science and Technology, 31, Pr. Krasnoyarsk worker, Krasnoyarsk, 660037, Russia

ARTICLE INFO

Keywords:
Low-carbon steel
Cross-helical rolling
Laser welding
Heat affected zone
Bainite
Microhardness

ABSTRACT

In this paper, the heat affected zone (HAZ) of laser welded joints of the X70 steel were studied by the transmission electron microscopy method. The effect of the initial microstructure (coarse-grained hot-rolled and fine-grained after cross-helical rolling) on the HAZ formation and the mechanical characteristics of the welded joints were shown. It was found that the microstructure in the inter-critical HAZ of the steel after cross-helical rolling was more dispersed, homogeneous, and uniform compared to that of the coarse-grained hot-rolled one due to the initial fine-grained ferrite-bainitic-pearlite microstructure and the absence of pronounced ferrite-pearlite banding in the base metal. The character of the microhardness value distribution in the HAZ of the steel after cross-helical rolling was smooth with the gradual decrease from 370 down to 185 HV as shifted towards the base metal. In the HAZ of the coarse-grained hot-rolled steel, the heterogeneous microhardness value (up to 640–670 HV) distribution was revealed. The reason was the upper degenerate bainite microstructure with high residual stresses, characterized by laths up to 2.0–2.5 μm long and a high martensitic-austenitic constituent fraction (10–16%) of a slender shape along the boundaries of bainite laths. The conclusion was drawn that one of the ways to reduce the brittleness of the laser welded joints could be using the initially fine-grained steels possessing the homogeneous (mainly bainitic) microstructure.

1. Introduction

Various factors play a role in the formation of the microstructure and the mechanical properties of welded joints of low-carbon microalloyed steels. The main ones are the level of carbon and alloying elements, the welding process conditions (the welding method, and its energy parameters), as well as the initial microstructure and the phase composition of the steel. In the fusion zone (FZ), the metal is overheated significantly above the A_{c3} critical point. This causes the complete austenite homogenization, followed by rapid cooling from high temperatures. As a result, it is difficult to control the microstructure in the FZ by changing the above factors. This is possible only in limited cases (for example, partially by varying the welding parameters). More complex microstructure transformations occur in the heat affected zone (HAZ) during the welding thermal cycles. The interest in the study of this zone is determined by the possibility to control its structure, which often determines the properties of the entire welded joint.

To date, a lot of data have been published on dependences of low-carbon steel HAZ formation patterns from various parameters [1–19]. A series of studies has been carried out to investigate the effect of microalloying elements on the formed HAZ microstructure [1–6]. They enable to control the phase transformation points, the type of obtained bainitic microstructures, as well as volume fractions and sizes of second phases (carbides and the brittle martensitic-austenitic (M-A)

* Corresponding author. Institute of Strength Physics and Materials Science of Siberian Branch Russian Academy of Sciences, 2/4, Pr. Akademicheskii, Tomsk, 634055, Russia.
E-mail address: mirantil@sibmail.com (A.I. Gordienko).

https://doi.org/10.1016/j.msea.2020.140075
Received 23 June 2020; Received in revised form 5 August 2020; Accepted 7 August 2020
Available online 10 August 2020

Table 1
The chemical composition of the X70 low-carbon microalloyed steel.

Element	C	Mn	V	Nb	Si	Ti	Cu	Al	P	S
Content, wt. %	0.13	1.6	0.05	0.04	0.4	0.05	0.3	0.03	0.013	0.01

component). The formation of carbonitrides affects grain sizes after heating and cooling cycles. Thus, it has been shown in Ref. [2–4] that doping with aluminum, molybdenum, and nickel has resulted in the formation of a homogeneous HAZ microstructure, as well as contributed to a decrease in the M-A constituent fraction and its sizes. As a result, the metal toughness has been improved.

Applying different welding methods and varying their energy parameters enable to control heat input levels and HAZ cooling rates. Accordingly, its dimensions, residual stresses, and the microstructure can be changed. A wide range of the microstructures can be formed (from ferritic-pearlitic to bainitic-martensitic) that directly affect the mechanical properties of the welded joints [6–13]. It has been shown that the use of laser welding results in narrower seams compared to that for arc welding methods. Typically, the shape factor (the ratio of the penetration depth to the weld width) is more than one [13]. In addition, strength of the laser welded joints of low-carbon steels remains at the base metal (BM) levels [11]. However, disperse lath microstructures, characterized by increased microhardness [9,10,12] and low fracture toughness [12], are formed due to high cooling rates upon laser welding.

Another way to control the microstructure and the properties of the HAZ is to change the initial steel microstructure [14–19]. It has been found that the fine-grained one promotes the formation of more ductile phases and improves impact toughness of the weld metal [14,15]. The non-uniform carbon distribution in steels also affects the formed microstructure in the HAZ upon rapid cooling after thermal exposure [16,17]. It has been shown that the microstructure and the M-A constituent fraction depend on the volume fraction and the sizes of perlite grains in the BM [17]. Thus, it is possible to predict the HAZ microstructure already at the stage of choosing steel with predefined properties. However, few results have been published on the dependence of the HAZ microstructure from the initial steel one. From a practical point of view, it is important to investigate the possibility of reducing the brittleness of laser welds by changing the initial steel microstructure.

One of the methods to improve the microstructure of steels is cross-helical rolling, which is applied for piercing and rolling of pipe workpieces. Due to their rotational-translational movement, higher shear strains are achieved in the bar surface layer as compared with conventional rolling processes. This contributes to the metal microstructure refinement. In Refs. [20,21], it has been shown that cross-helical rolling enables to significantly improve fracture toughness and reduce the brittle-ductile transition temperature of mild steel. Based on this fact, cross-helically rolled steel samples were welded.

The aim of this paper has been to study the HAZ microstructure and the mechanical properties of a laser welded joint of the X70 low-carbon microalloyed steel after cross-helical rolling and to compare with those of the coarse-grained hot-rolled one.

2. Experimental procedure

In the present studies, the X70 low carbon microalloyed steel (Table 1) after cross-helical rolling was investigated. Then, the obtained data were compared with the results of the similar author's studies of the X70 coarse-grained hot-rolled steel [12].

Cross-helical rolling was done using an "CHR 14–40" three-roll mini-mill from a temperature of 920°C for six passes. The process began near the A_{r3} critical point and completed in the upper part of the ($\gamma+\alpha$)-region. The phase transformation temperatures (A_{c1} = 788 °C and A_{c3} = 892 °C upon heating, as well as A_{r1} = 767 °C and A_{r3} = 814 °C upon cooling) were determined for the X70 coarse-grained hot-rolled steel by a "STA 409 PC Luxx" synchronous thermal analyzer. The start bainitic transformation temperature B_s was 569 °C.

Plates with dimensions of 55 × 55 × 1.2 mm were cut from a bar along the cross-helical rolling direction. Then, they were welded perpendicular to the longitudinal axis using a "Siberia-1" automated

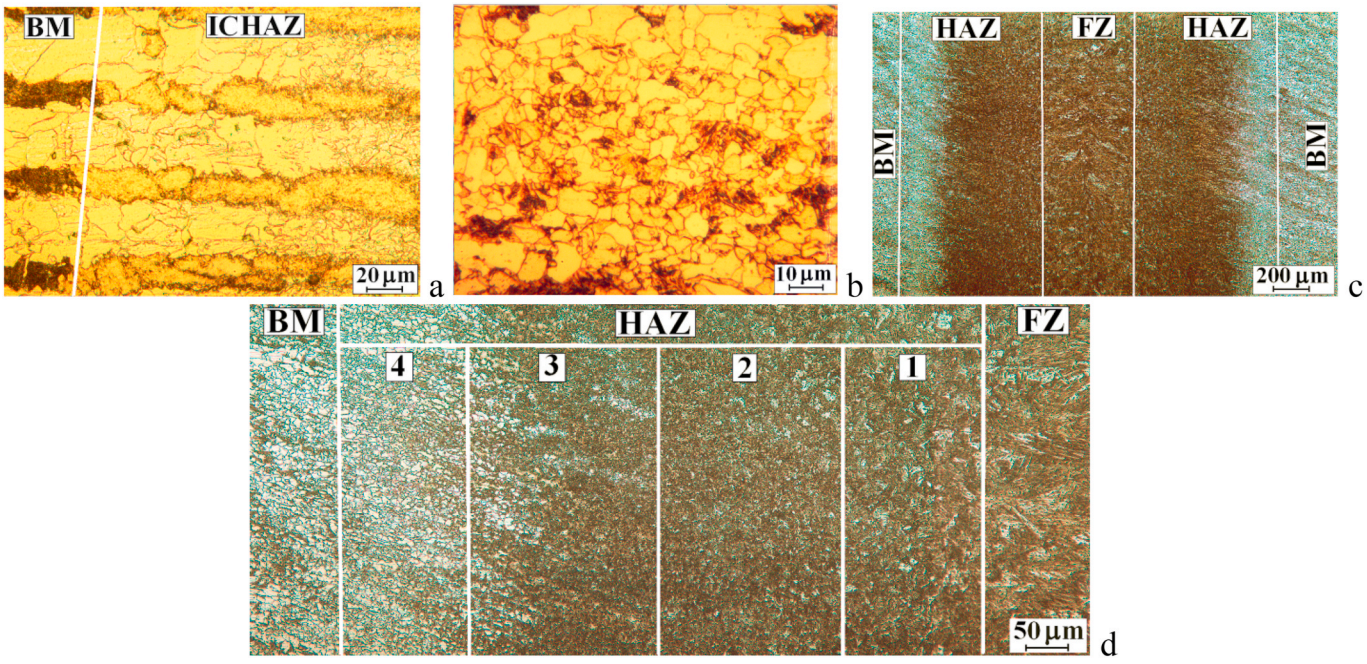

Fig. 1. The BM and HAZ microstructures of the X70 steel: hot-rolled (a); after cross-helical rolling (b); the weld zone (c) and its HAZ (d) of the steel after cross-helical rolling.

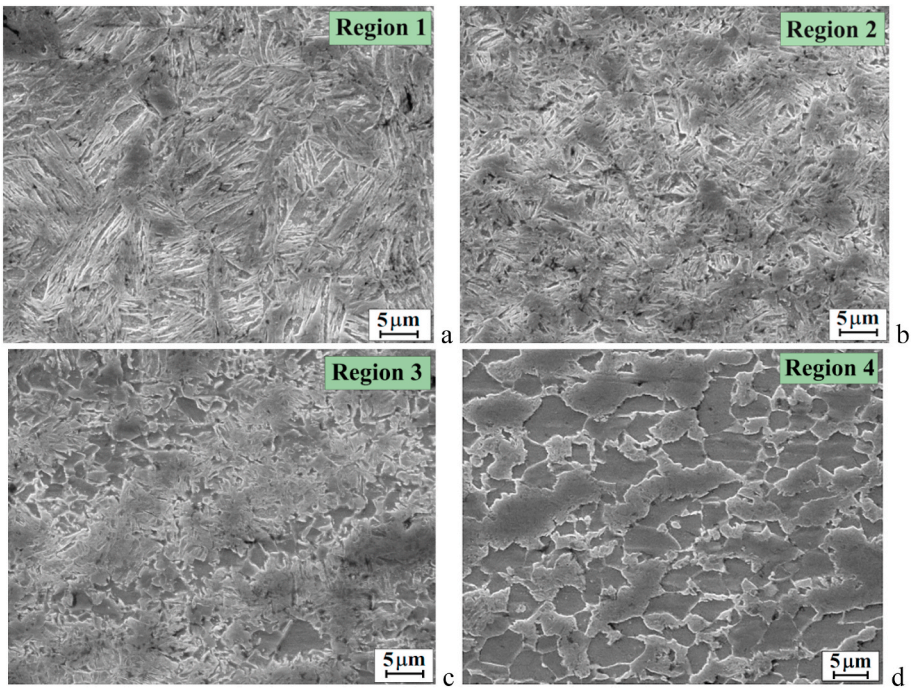

Fig. 2. SEM images of the metal microstructure in different parts of the heat-affected zone of the steel after cross-helical rolling.

facility included a CO_2 continuous laser with a wavelength of 10.6 μm and a power of up to 8 kW [22]. The weld zone and the root were shielded with an inert gas (helium). A laser beam was focused 2 mm underneath the plate surfaces. Keyhole welding was carried out in one pass at a power of 1.2 kW and welding speed of 1 m/min.

Samples for metallographic studies were prepared by etching in a 3% solution of nitric acid in alcohol. Microstructures in the weld zone were examined using a "Zeiss Axiovert 25" optical microscope (OM), a "Philips SEM 515" scanning electron microscope (SEM) and an "HT-7700" transmission electron microscope (TEM). The average grain size was determined using OM and TEM images by the average grain intercept (AGI) method. Local microstructural studies of various HAZ regions were carried out using foils cut by an "FIB2100" focused ion beam (FIB) system. TEM studies were added to the article in response to a reviewer comment. But the authors forgot to add a description of TEM studies to the section Experimental procedure.

Vickers microhardness values were obtained along the longitudinal weld axis by a "PMT-3" setup at a load of 100 g. At least five

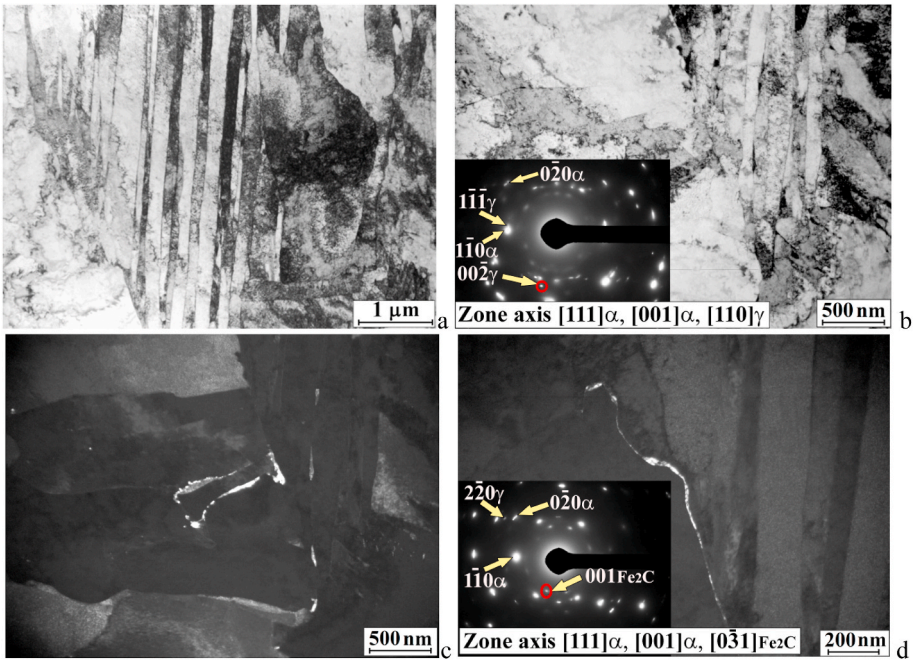

Fig. 3. TEM images of the FG HAZ: a, b – bright field images with the corresponding microdiffraction pattern (b, the arrows indicate the reflexes of the [111]α, [001]α, and [110]γ zones); c – the dark field image in the $00\bar{2}$ reflex from γ-Fe; d – the dark field image in the 001 reflex from Fe_2C (the reflexes of the [111]α, [001]α, and $[0\bar{3}1]Fe_2C$ zones are indicated in the microdiffraction pattern).

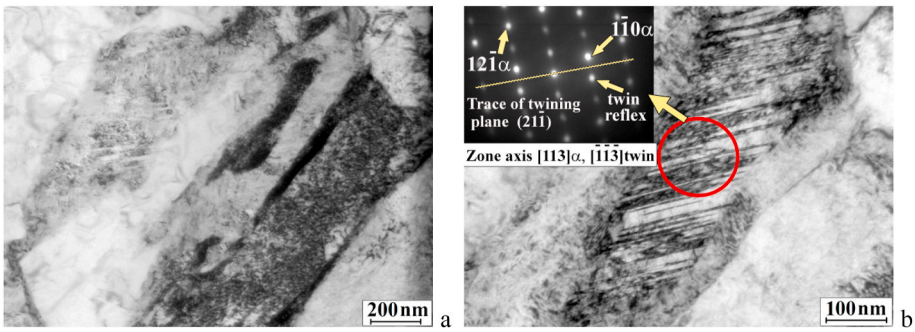

Fig. 4. Bright field TEM images of the bainitic microstructure (a, b) in the FG HAZ and the diffraction pattern of the area marked with a red circle (b). (For interpretation of the references to colour in this figure legend, the reader is referred to the Web version of this article.)

measurements were performed on one test point. Uniaxial static tensile tests were carried out using a "Polyani" facility with automatic recording of loading curves at room temperature and a load rate of ~0.002 mm/s "Dog-bone" samples were cut by electric discharge machining. Their thinned parts were $15 \times 3 \times 1$ mm^2. Welds were in the middle of the samples.

3. Results

3.1. Microstructural studies

3.1.1. Optical metallography and scanning electron microscopy

In [12], it was shown that the ferrite-pearlite microstructure with the pronounced banding of structural elements was formed in the X70 coarse-grained hot-rolled steel (Fig. 1, a). The average size of ferrite grains was 12 μm, their volume fraction was 20%. Vanadium carbides (VC) with sizes of 5–25 nm were inside them.

As a result of cross-helical rolling, the X70 steel microstructure became finer (Fig. 1, b), the brittle pearlite component fraction decreased down to 11%, and the bainitic component had been formed [20,21]. The bainite volume fraction in the microstructure was 15%. The average size of ferrite grains decreased down to 5 μm, and they were strengthened with Fe_3C and VC carbide particles.

The laser weld width of the X70 steel after cross-helical rolling was about 2.2 mm (Fig. 1, c). Clear contours of the FZ with a width of approximately 0.55 mm and the HAZ located to the left and right of the FZ were found in the weld zone. The lath martensite dendritic microstructure had been formed in the FZ.

Four regions were observed in the HAZ (Fig. 1, d). The coarse-grained (CG) region 1 (Fig. 2, a) was adjacent to the FZ and corresponded to the CG HAZ. Its width was 180 μm on each side of the FZ. The microstructure in this region was of the bainitic-martensitic type, laths were limited by the boundaries of prior austenite grains. The microstructure of the next region 2 with a width of 230 μm (Fig. 2, b) was similar to the region 1, but was more dispersed. It corresponded to the fine-grained (FG) HAZ. In the inter-critical (IC) region 3 with a width of 240 μm (IC HAZ), alternating light and dark areas were detected (Fig. 2, c). The light areas corresponded to fine-grained ferrite, and the dark ones possessed the bainitic microstructure. The average ferrite grain size was 6.5 μm. The microstructure of the region 4 with a width of approximately 150 μm was represented by ferrite and bainite quasi-equiaxed grains (Fig. 2, d). The size of ferrite grains was ≈6.5 μm; the dimensions of bainitic ones were in the range from 1.5 to 2.0 μm. The initial ferrite-pearlite-bainitic microstructure was in the transition area near the BM.

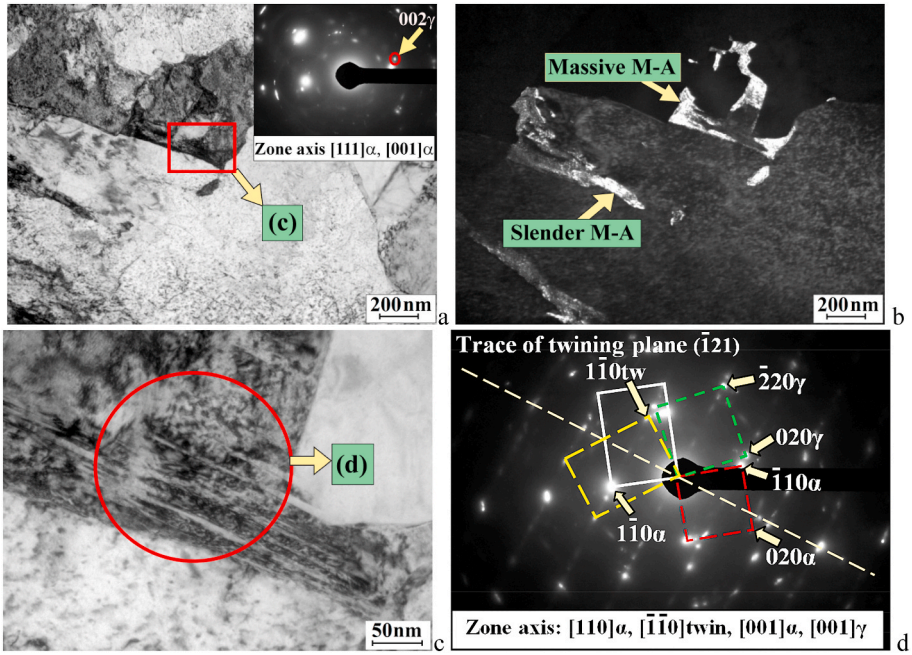

Fig. 5. TEM images of the FG HAZ: a, c – the bright field images of the M-A constituent area; b – the dark field image in the 002 reflex from γ-Fe; d – the microdiffraction pattern from the region indicated in Fig. 5, c.

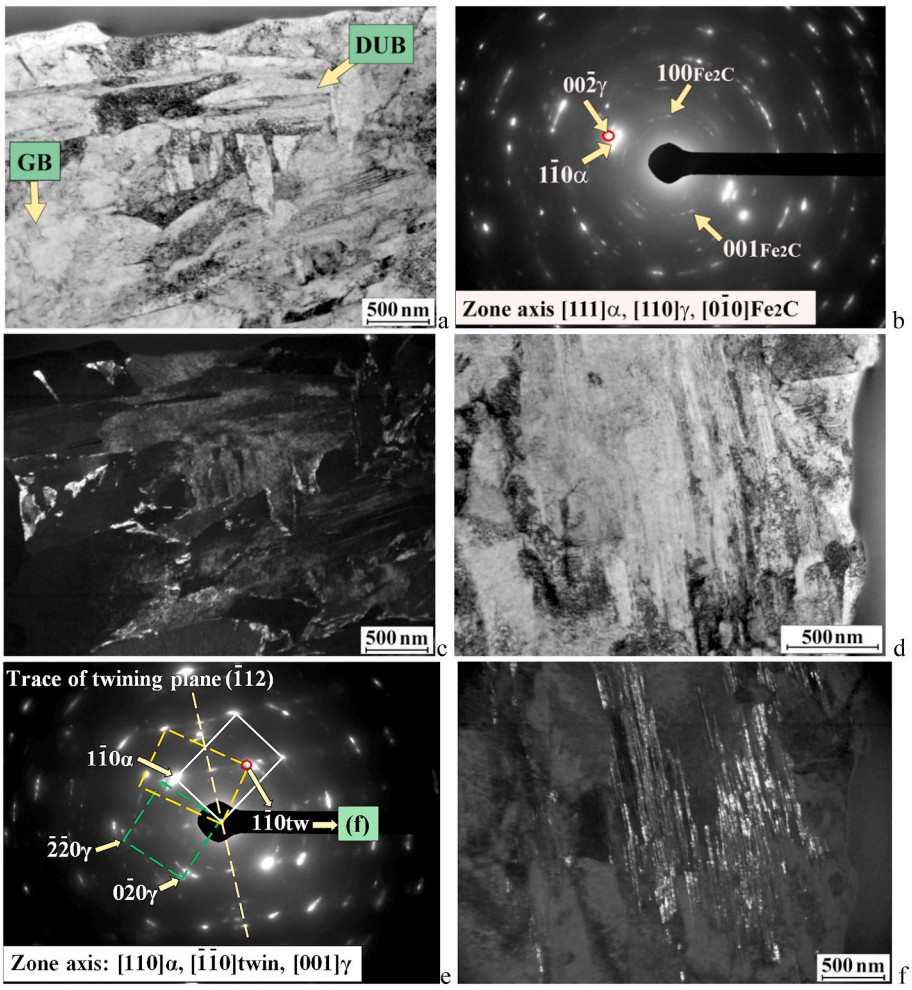

Fig. 6. TEM images of the IC HAZ: a, d – the bright field images of the bainitic microstructure; b – the microdiffraction pattern, the arrows indicate reflexes of the [111] α, [110]γ, and [0$\bar{1}$0]Fe_2C zones; c – the dark field images in the 00$\bar{2}$ reflex from γ-Fe; e – the microdiffraction pattern from the twin martensite region, the arrows indicate the reflexes of the [110]α, [$\bar{1}\bar{1}$0]twin and [001]γ zones; f – the dark-field image in the twin reflex.

3.1.2. Transmission electron microscopy

According to the results of optical microscopy, it was found that the bainitic microstructure was different in various HAZ regions. The TEM investigations were performed for their detailed study in each region. Since the microstructures in the CG HAZ and the FG HAZ were qualitatively similar and differed only in the sizes of structural elements, the results of the FG HAZ studies were solely presented. In the FG HAZ, grains with long slats typical of lath martensite were detected (Fig. 3a and b). Their length reached 5 μm, which was commensurate with the prior grain sizes. The width of martensite laths varied in the range from 40 to 500 nm. Particles of carbides or residual austenite were mostly absent between the laths. Only in a few cases, areas of residual austenite with a width of 20–70 nm and a length of 150–500 nm were between the laths and near the boundaries of prior austenitic grain (Fig. 3, c), which was typical for the slender type M-A constituent [23]. Areas of [110]γ austenite and [111]α ferrite were determined in the diffraction patterns near the boundaries of austenitic grains (at the acute-angled ends of martensite laths), that indicated the fulfillment of the Kurdjumov-Sachs orientation relationship (Fig. 3, b). This confirmed the fact of the martensitic transformation. Fe_2C carbide interlayers 10–15 nm thick were also found at the boundaries of prior austenitic grains (Fig. 3, d).

In addition to martensitic grains, bainitic ones of the (basically) lath morphology were found in the FG HAZ (Fig. 4, a). The thickness of bainite laths was 200–350 nm, although thinner ones with a thickness of 55–220 nm were also found. Between bainite-ferrite laths, areas of the M-A constituent in the form of twin martensite were found (Fig. 4, b). This microstructure was characteristic of degenerate upper bainite [24]. It should be noted that the twin martensite areas were oblong (the slender type) with a length of 150–600 nm and a width of 40–200 nm. The thickness of twin martensite laths was 5–10 nm.

In the bainitic microstructure, the slender type M-A constituent areas in the form of residual austenite were also found between the laths. They mainly included layers with a length of 400–500 nm and a width of 30–50 nm (Fig. 5a and b).

Other M-A constituent areas of more complex configurations were at the junctions of some grains (Fig. 5, a and c). The M-A constituent of a massive type included sections of residual austenite with a width of 50–150 nm (Fig. 5, b) and twin martensite with a lath width of 5 nm (Fig. 5c and d). The average residual austenite fraction in the FG HAZ bainitic microstructure was about 3%. It should be noted that the assessment of the residual austenite fraction was carried out approximately. It was counted only in the specific bainitic areas under consideration, and not over the entire HAZ area.

In the IC HAZ (region 3), the bainitic microstructure corresponded to the dark areas in the optical images (Fig. 1, d). Bainite was in the form of parallel bainite-ferrite laths grouped into small packets misoriented relat ive to each other (Fig. 6, a). The lath thickness varied in the range from 50 up to 200 nm and their length was from 0.5 up to 3.4 μm. At the boundaries of bainitic packets and between laths, sections of the M-A constituent, predominantly of the slender type, were found (Fig. 6b and

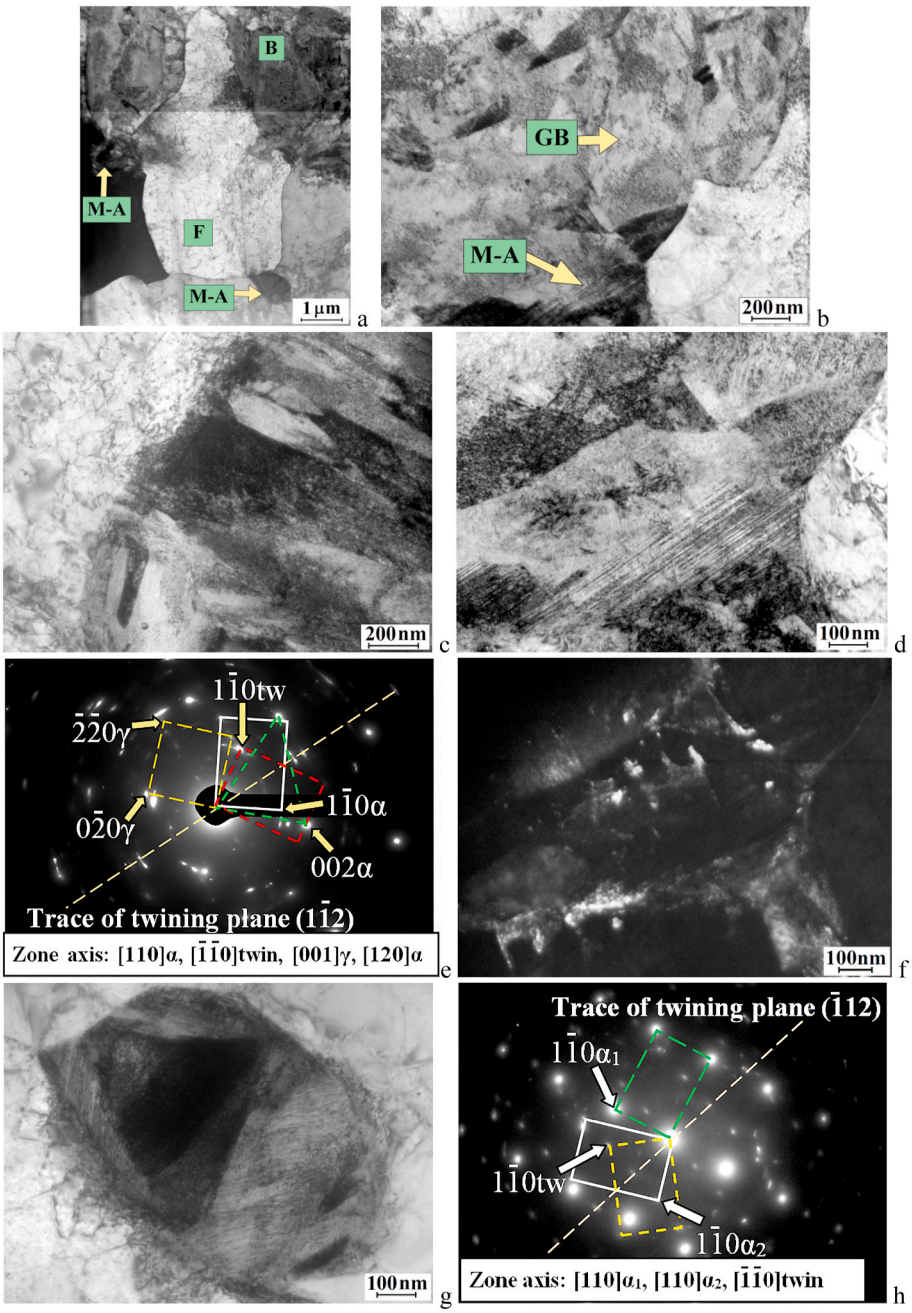

Fig. 7. TEM images of the region 4 HAZ: a–d – the bright field images of the bainitic microstructure; e – the microdiffraction pattern from the area shown in Fig. 7, d: the arrows indicate reflexes of the [110]α, [001]γ, [$\bar{1}\bar{1}$0]twin and [120]α zones; f – the dark field images in the 0$\bar{2}$0 reflex from γ-Fe; g – the bright field image of the M-A constituent; h – the corresponding microdiffraction pattern.

c). Interlayers of residual austenite 20–40 nm wide and 150–400 nm long were also observed. This microstructure corresponded to upper degenerate bainite. Some granular bainite (GB) and Fe_2C carbide particles were also in the IC HAZ microstructure. The residual austenite fraction in the IC HAZ bainitic areas was 9%.

The IC HAZ also contained the M-A constituent areas of a massive type in the form of twin martensite (Fig. 6, d–f) with a length of 1.2–1.6 μm and a width of 0.5 μm. The lath thickness in twins was 5–10 nm. In such areas, residual austenite layers 20–40 nm thick were located next to martensite twins.

In the region 4 HAZ microstructure, ferritic grains of 3–4 μm in size and darker bainitic grains of 1.5–1.7 μm were found (Fig. 7, a). A more detailed examination of the microstructure revealed granular bainite grains with unclear boundaries (Fig. 7, b), as well as sections of the lath bainite morphology (Fig. 7, c). The width of bainitic ferrite laths was 60–250 nm. The formation of unclear bainite sections was associated with nonequilibrium conditions upon cooling after welding and a short duration at temperatures sufficient for the bainitic transformation. The granular bainite block sizes ranged from 0.5 to 1.2 μm. At the granular bainite grain boundaries, the M-A constituent areas were located that consisted of twin martensite packets and residual austenite sections (Fig. 7, d–f). The widths of twin martensite packets were 250 nm and their lengths were 600 nm. The thicknesses of twin martensite laths were 5–10 nm. The slender-shape residual austenite layers were 10–20 nm thick and up to 200 nm long.

At the boundaries of ferritic and bainitic grains, there were larger sections of the M-A constituent of a massive shape with a length of 1000 nm and a width of 600 nm (Fig. 7g and h). Inside them, the M-A

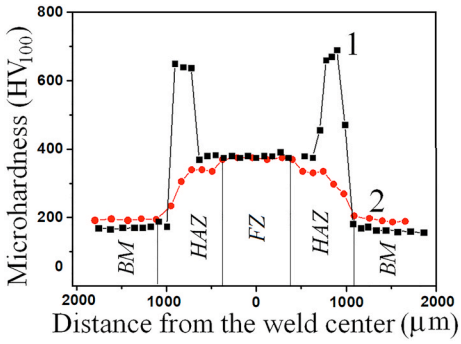

Fig. 8. The microhardness value distributions in the X70 steel welds: 1 – hot-rolled; 2 – after cross-helical rolling.

Table 2
The mechanical properties of the X70 steel.

Steel	YS, MPa	UTS, MPa	ε, %
Hot-rolled, base metal	380	650	23.7
Hot-rolled, weld metal	390	600 ↓**7%**	21 ↓**11%**
After cross-helical rolling, base metal	435	760	24
After cross-helical rolling, weld metal	445	690 ↓**9%**	19 ↓**20%**

constituent was presented as twin martensite sections.

It can be concluded from the analysis of the microstructure in the region 4 HAZ that the M-A constituent was predominantly represented by twin martensite areas. The fraction of residual austenite sections in the bainitic areas was 2–3%.

3.2. Mechanical tests

3.2.1. Microhardness

Fig. 8 shows the microhardness distribution curves for the X70 steel welded samples in the hot-rolled state (curve 1) [12] and after cross-helical rolling (curve 2). Compared to the BM microhardness values of 170–185 HV, they increased in the weld region. Microhardness of the both steels increased up to 380 HV in the FZ. The heterogeneous microhardness value distribution was revealed in the HAZ of the hot-rolled steel. A significant increase in the microhardness values up to 640–670 HV was observed on the curve. In the steel after cross-helical rolling, the microhardness value distribution curve was smoother in the HAZ with the gradual decreasing down to the BM level. The maximum microhardness values were observed in the both CG HAZ and FG HAZ regions (370 HV and 340 HV, respectively). In contrast, the maximum values were found in the IC HAZ of the hot-rolled steel.

3.2.2. Tensile behavior

As was shown in Ref. [12], tensile strength of the X70 hot-rolled steel welded samples decreased insignificantly by 7%, and ductility by 11% compared with those of the BM (Table 2). These parameters were reduced by 9% and 20%, respectively, for the steel after cross-helical rolling.

4. Discussion

Upon laser welding of the X70 steel after cross-helical rolling, the narrow weld had been formed. Four regions were found in the HAZ. The phase composition, the size, and the morphology of structural elements were different in each region because the thermal cycles (the heating and cooling rates) had been various as well.

Table 3 shows the bainite structural characteristics in different regions of the HAZ. A comparison of three HAZ regions of the X70 steel after cross-helical rolling showed that in the FG HAZ (region 2), in which the martensite and bainite microstructures had been formed, upper bainite and martensite laths were wider than that in other HAZ regions. This was due to higher heating temperatures (the lower region of the γ phase existence) and large austenitic grains, as a result, as well as the high cooling rate. The M-A constituent was the slender type, while the residual austenite fraction was 3%. In addition, there were few elongated twin martensite sections.

When the metal had been heated up to the range of the inter-critical temperatures, the carbon concentration had been inhomogeneous in the IC HAZ (region 3) due to the formation of ferrite and austenite sections depleted and enriched with carbon. This fact was noted in Ref. [16]. After the bainitic transformation in austenite areas with the locally increased carbon content, the M-A constituent fraction in the microstructure was significantly enhanced. The residual austenite fraction rose up to 9%, and the sizes of the twin martensite areas increased up to (500–700) × 1600 nm.

In the region 4 H AZ, ferritic grains, granular and lath bainite were present without pearlite inclusions. This testified to the metal heating up to the (γ + α) region temperatures. The metal temperatures closer to the A_{c1} critical point resulted in the carbon content increasing in austenite formed from pearlite [25]. In the areas enriched with carbon, the M_s point of the martensitic transformation had shifted to the region of lower temperatures. Therefore, the M-A constituent was predominantly represented by twin martensite sections in the region 4 HAZ (Fig. 7, g), while the residual austenite fraction was 2–3%. However, the M-A constituent fraction was less in the region 4 HAZ than that in the in the region 3. The obtained data were consistent with the results of [26,27], in which it was found that the largest amount of the M-A constituent had been formed at temperatures of 15–50 °C above the A_{c1} critical point. The authors of [28] showed that austenite sections supersaturated with carbon had possessed only the martensitic transformation upon heating up to the A_{c1} critical point region and subsequent rapid cooling. With an increase in the heating temperature to the mid-range of the (γ + α) region, the transformed austenite fraction increased and the carbon concentration decreased inside it. This caused the bainitic transformation upon cooling, diffusion of carbon into residual austenite, and the subsequent martensitic transformation. The high M-A constituent fraction

Table 3
The structural component sizes in various HAZ regions of the X70 steel.

HAZ region		h_B, nm	h_{RA}, nm	l_{RA}, nm	V_{RA}, %	$h_{area\ twin}$, nm	h_{twin}, nm
After cross-helical rolling	FG HAZ	200–350	30–50	400–500	3	(40–200) × (150–600)	5–10
	IC HAZ (region 3)	50–200	20–40	150–400	9	(500–700) × up to 1600	5–10
	IC HAZ (region 4)	60–250 GB = 500–1200	10–20	30–200	2–3	250 × (500–600) (up to 600 × 1000)	5–10
Hot-rolled	IC HAZ [12]	140–300	Slender 20–60 Massive 80–120	100–800	10–16	(170–200) × 370	5–7

h_B is the width of bainitic ferrite laths; h_{RA} is the thickness of the residual austenite plates; l_{RA} is the length of residual austenite sections; V_{RA} is the residual austenite fraction area; $h_{area\ twin}$ is the dimensions of twin martensite areas; h_{twin} is the thickness of twins; GB is granular bainite.

had been formed in the microstructure as a result, while it was lower after heating up to the A_{c1} region. It was also shown in Ref. [29] that the sizes and the fraction of the M-A constituent reduced with the carbon content increasing in the formed austenite microstructure due to its stabilization and the M_s point decreasing.

In the weld zone of the steel after cross-helical rolling, the maximum microhardness values were observed in the FZ (Fig. 8) because of the formed martensitic microstructure with high residual stresses. In the HAZ, they were lower and gradually decreased due to the shifting from the martensitic microstructure to the ferritic-bainitic one.

In contrast, the maximum microhardness was observed in the IC HAZ of the X70 hot-rolled steel, but not in the FZ [12]. In this case, the microhardness values reached 640–670 HV (Fig. 8). It was shown that the high microhardness values in the IC HAZ were due to formed upper degenerate bainite with high residual stresses. It was characterized by long laths up to 2.0–2.5 μm and the high M-A constituent fraction (10–16%) of the slender shape along the boundaries of bainite laths. The BM of the X70 hot-rolled steel possessed large ferritic and pearlitic grains with the sizes of about 12 μm and pronounced pearlitic bands [12] (Fig. 1, a). As a result, the pearlite areas had transformed into the γ phase upon the IC HAZ metal heating. After its cooling, granular bainite formed at the boundaries of prior pearlite areas in addition to upper bainite laths. This testified to the fact that partial carbon diffusion had occurred into neighboring ferrite areas upon cooling. As a result, the carbon concentration decreased at the boundaries of prior pearlite areas. As noted above, the bainitic transformation rate was higher with a decrease in the carbon content. The start bainitic transformation point had increased and granular bainite had formed [30]. However, most of prior pearlite areas possessed a high carbon concentration due to the limited carbon diffusion process duration. Inside them, degenerate upper bainite laths with the high M-A constituent fraction had been formed. Therefore, high microhardness values were observed in this region.

In the steel after cross-helical rolling, ferrite and pearlite grains were more dispersed with sizes of about 5 μm (Fig. 1, b). Moreover, bainitic grains were in the microstructure. The carbon concentration was more uniform inside them compared to that of the ferrite-pearlite microstructure. As it was shown in Ref. [31], the lower were the austenitic grain sizes, the less were bainitic grains after the microstructure transformations upon welding. Therefore, the microstructure was finer in the IC HAZ of the X70 steel after cross-helical rolling. The structural element banding was weakly expressed. This resulted in the more uniform microstructure, compared with that of the hot-rolled steel [19]. The smaller were the pearlite grain sizes, the easier carbon diffused into neighboring ferrite grains, and the smaller were lath areas with high residual stresses. Lath bainite areas were intertwined with granular bainite (Fig. 6, a). It is known [32] that small austenitic grains reduced the steel tendency to be quenched upon welding. As a result, the lower microhardness level was observed in the HAZ compared to that of the hot-rolled steel.

Thus, the microstructure in the HAZ of the X70 steel after cross-helical rolling was characterized by greater dispersion and formed granular bainite in addition to upper bainite laths, as well as the lower M-A constituent fraction and its smaller sizes compared to the coarse-grained hot-rolled steel. All of these provided the lower microhardness level and the more uniform value distribution in the HAZ. Therefore, one of the ways to reduce the brittleness of the laser welded joints could be using the initially fine-grained steels possessing homogeneous (mainly bainitic) microstructure.

5. Conclusions

1. As a result of laser welding of the X70 steel after cross-helical rolling, four regions were observed in the HAZ. They were characterized by the size and the morphology of microstructural components. In the fine-grained region (FG HAZ), martensite and upper degenerate bainite had been formed. Between laths, the martensitic-austenitic (M-A) constituent sections of the slender type were located. They consisted of residual austenite and twin martensite. In the middle of the inter-critical HAZ (IC HAZ), ferrite, upper degenerate bainite, and the small granular bainite fraction were found, in which the M-A constituent of the slender shape (in the form of residual austenite) and the massive one (in the form of twin martensite) were present. On the IC HAZ edge, bainite of the predominantly granular morphology had been formed with the M-A constituent regions constituting the massive shape in the form of twin martensite.
2. It was shown that the microstructure in the IC HAZ of the X70 steel after cross-helical rolling was more dispersed, homogeneous, and uniform compared to that of the hot-rolled steel due to the initial fine-grained ferrite-bainitic-pearlite microstructure and the absence of pronounced ferrite-pearlite banding in the BM.
3. Unlike the hot-rolled X70 steel, the character of the microhardness value distribution in the HAZ of the one after cross-helical rolling was smooth with the gradual decrease from 370 down to 185 HV as shifted towards the BM. This was facilitated by the formed bainitic structure with lower stresses and a smaller proportion and dimensions of the M-A component.

Data availability

The raw/processed data required to reproduce these findings cannot be shared at this time as the data also forms part of an ongoing study.

Declaration of competing interest

The authors declare that they have no known competing financial interests or personal relationships that could have appeared to influence the work reported in this paper.

Acknowledgments

Microstructural studies and mechanical tests of laser welds were performed within the frame of the Fundamental Research Program of the State Academies of Sciences for 2013–2020, line of research III.23.1.1. Part of the research related to the selection of optimal laser welding parameters for low carbon steels was carried out within Basic State Project No. AAAA-A17-117030610122-6.

TEM studies were carried out in Center of Federal Research Center of Kirensky Institute of Physics SB RAS. The authors are grateful to I.P. Mishin. for assistance in cross-helical rolling of the steel.

References

[1] Y. You, C. Shang, N. Wenjin, S. Subramanian, Investigation on the microstructure and toughness of coarse grained heat affected zone in X-100 multi-phase pipeline steel with high Nb content, Mater. Sci. Eng. 558 (2012) 692–701, https://doi.org/10.1016/j.msea.2012.08.077.

[2] L. Yu, H.H. Wang, X.L. Wang, G. Huang, T.P. Hou, K.M. Wu, Improvement of impact toughness of simulated heat affected zone by addition of aluminium, Mater. Sci. Technol. 30 (2014) 1951–1958, https://doi.org/10.1179/1743284714Y.0000000602.

[3] B.L. Xiao-wei Chen, Gui-ying Qiao, Xiu-lin Han, Xu Wang, Fu-ren Xiao, Effects of Mo, Cr and Nb on microstructure and mechanical properties of heat affected zone for Nb-bearing X80 pipeline steels, Mater. Des. 53 (2014) 888–901.

[4] Y. You, C. Shang, S. Subramanian, Effect of Ni addition on toughness and microstructure evolution in coarse grain heat affected zone, Met. Mater. Int. 20 (2014) 659–668, https://doi.org/10.1007/s12540-014-4011-4.

[5] R. Taillard, P. Verrier, T. Maurickx, J. Foct, Effect of silicon on CGHAZ toughness and microstructure of microalloyed steels, Metall. Mater. Trans. 26 (1995) 447–457, https://doi.org/10.1007/BF02664681.

[6] Z. Zhu, L. Kuzmikova, H. Li, F. Barbaro, The effect of chemical composition on microstructure and properties of intercritically reheated coarse-grained heat-affected zone in X70 steels, in: Metall. Mater. Trans. B Process Metall. Mater. Process. Sci., 2014, pp. 229–235, https://doi.org/10.1007/s11663-013-0008-5.

[7] D. Kong, C. Ye, W. Guo, Y. Wu, D. Long, Microstructures and plane energy spectra of X80 pipeline steel welded joints by submerged arc automatic welding, J. Wuhan Univ. Technol.-Materials Sci. Ed. 29 (2014) 1265–1269, https://doi.org/10.1007/s11595-014-1079-0.

[8] A.E. Amer, M.Y. Koo, K.H. Lee, S.H. Kim, S.H. Hong, Effect of welding heat input on microstructure and mechanical properties of simulated HAZ in Cu containing microalloyed steel, J. Mater. Sci. 45 (2010) 1248–1254, https://doi.org/10.1007/s10853-009-4074-7.
[9] S. Němeček, T. Mužík, M. Míšek, Differences between laser and arc welding of HSS steels, Phys. Procedia. 39 (2012) 67–74, https://doi.org/10.1016/j.phpro.2012.10.015.
[10] J.H. Lee, S.H. Park, H.S. Kwon, G.S. Kim, C.S. Lee, Laser, tungsten inert gas, and metal active gas welding of DP780 steel: comparison of hardness, tensile properties and fatigue resistance, Mater. Des. 64 (2014) 559–565, https://doi.org/10.1016/j.matdes.2014.07.065.
[11] W. Li, L. Ma, P. Peng, Q. Jia, Z. Wan, Y. Zhu, W. Guo, Microstructural evolution and deformation behavior of fiber laser welded QP980 steel joint, Mater. Sci. Eng. 717 (2018) 124–133, https://doi.org/10.1016/j.msea.2018.01.050.
[12] L.S. Derevyagina, A.I. Gordienko, Orishich, A.G. Malikov, N.S. Surikova, M. N. Volochaev, Microstructure of intercritical heat affected zone and toughness of microalloyed steel laser welds, Mater. Sci. Eng. 770 (2020) 138522, https://doi.org/10.1016/j.msea.2019.138522.
[13] N.B. Pugacheva, E.B. Trushina, N.P. Antenorova, Effect of laser processing on the microstructure of a structural low-carbon steel, Russ. Metall. (2014) 569–575, https://doi.org/10.1134/S0036029514070118, 2014.
[14] M. Eroglu, M. Aksoy, Effect of initial grain size on microstructure and toughness of intercritical heat-affected zone of a low carbon steel, Mater. Sci. Eng. 286 (2000) 289–297, https://doi.org/10.1016/S0921-5093(00)00801-7.
[15] X. Li, X. Ma, S.V. Subramanian, C. Shang, R.D.K. Misra, Influence of prior austenite grain size on martensite–austenite constituent and toughness in the heat affected zone of 700MPa high strength linepipe steel, Mater. Sci. Eng. 616 (2014) 141–147, https://doi.org/10.1016/j.msea.2014.07.100.
[16] T. Lolla, S.S. Babu, S. Lalam, M. Manohar, Understanding the role of initial microstructure on intercritically reheated heat-affected zone microstructures and properties of microalloyed steels, in: ASM Proc. Int. Conf. Trends Weld. Res., 2013, pp. 34–42.
[17] O.M. Akselsen, J.K. Solberg, O. Grong, Effects of martensite-austenite (M-A) islands on intercritical heat-affected zone toughness of low carbon microalloyed steels, Scand. J. Metall. 17 (1988) 194–200.
[18] L. Lan, C. Qiu, D. Zhao, X. Gao, L. Du, Effect of reheat temperature on continuous cooling bainite transformation behavior in low carbon microalloyed steel, J. Mater. Sci. 48 (2013) 4356–4364, https://doi.org/10.1007/s10853-013-7251-7.
[19] K. Banerjee, Role of base metal microstructure on tensile properties and weldability of simulated continuously annealed advanced high strength steels, Int. J. Metall. Eng. 2 (2013) 100–110, https://doi.org/10.5923/j.ijmee.20130201.15.
[20] L.S. Derevyagina, A.I. Gordienko, Y.I. Pochivalov, A.S. Smirnova, Modification of the structure of low-carbon pipe steel by helical rolling, and the increase in its strength and cold resistance, Phys. Met. Metallogr. 119 (2018) 83–91, https://doi.org/10.1134/S0031918X18010076.
[21] V.E. Panin, L.S. Derevyagina, S.V. Panin, A.R. Shugurov, A.I. Gordienko, The role of nanoscale strain-induced defects in the sharp increase of low-temperature toughness in low-carbon and low-alloy steels, Mater. Sci. Eng. 768 (2019) 138491, https://doi.org/10.1016/j.msea.2019.138491.
[22] A. Malikov, N. Bulina, M. Sharafutdinov, A. Orishich, Study of the structure and phase composition of laser welded joints of Al-Cu-Li alloy under different heat treatment conditions, Int. J. Adv. Manuf. Technol. 104 (2019) 4313–4324, https://doi.org/10.1007/s00170-019-04286-w.
[23] X. Luo, X. Chen, T. Wang, S. Pan, Z. Wang, Effect of morphologies of martensite–austenite constituents on impact toughness in intercritically reheated coarse-grained heat-affected zone of HSLA steel, Mater. Sci. Eng. 710 (2018) 192–199, https://doi.org/10.1016/j.msea.2017.10.079.
[24] S. Zajac, V. Schwinnand, K.H. Tacke, Characterisation and quantification of complex bainitic microstructures in high and ultra-high strength linepipe steels, Mater. Sci. Forum 500–501 (2005) 387–394, https://doi.org/10.4028/www.scientific.net/msf.500-501.387.
[25] X. Li, Y. Fan, X. Ma, S.V. Subramanian, C. Shang, Influence of Martensite-Austenite constituents formed at different intercritical temperatures on toughness, Mater. Des. 67 (2015) 457–463, https://doi.org/10.1016/j.matdes.2014.10.028.
[26] E. Bonnevie, G. Ferrière, A. Ikhlef, D. Kaplan, J.M. Orain, Morphological aspects of martensite-austenite constituents in intercritical and coarse grain heat affected zones of structural steels, Mater. Sci. Eng. 385 (2004) 352–358, https://doi.org/10.1016/j.msea.2004.06.033.
[27] E. Bayraktar, D. Kaplan, Mechanical and metallurgical investigation of martensite-austenite constituents in simulated welding conditions, J. Mater. Process. Technol. 153–154 (2004) 87–92, https://doi.org/10.1016/j.jmatprotec.2004.04.021.
[28] Z. Li, X. Zhao, D. Shan, Impact toughness of subzones in the intercritical heat-affected zone of low-carbon bainitic steel, Materials 11 (2018), https://doi.org/10.3390/ma11060959.
[29] L. Yu, H.H. Wang, T.P. Hou, X.L. Wang, X.L. Wan, K.M. Wu, Characteristic of martensite–austenite constituents in coarse grained heat affected zone of hsla steel with varying al contents, Sci. Technol. Weld. Join. 19 (2014) 708–714, https://doi.org/10.1179/1362171814Y.0000000246.
[30] N. Takayama, G. Miyamoto, T. Furuhara, Chemistry and three-dimensional morphology of martensite-austenite constituent in the bainite structure of low-carbon low-alloy steels, Acta Mater. 145 (2018) 154–164, https://doi.org/10.1016/j.actamat.2017.11.036.
[31] X. Liang, A.J. Deardo, A study of the influence of thermomechanical controlled processing on the microstructure of bainite in high strength plate steel, Metall. Mater. Trans. A Phys. Metall. Mater. Sci. 45 (2014) 5173–5184, https://doi.org/10.1007/s11661-014-2444-5.
[32] P. Kirkwood, Enhancing the weldability of C-Mn pressure vessel steels — a tale of two elements, Energy Mater (2014) 61–70, https://doi.org/10.1007/978-3-319-48765-6_7.